ELEKTRİK, VOL.6, NO.3, 1998, ©TÜBİTAK

Functional Radionuclide İmaging Algorithm Based On The Appended Curve Deconvolution Technique And Its Use In The Diagnosis Of Renovascular Hypertension

İrfan Karagöz
Biomedical and Clinical Engineering Center,
Gülhane Military Medical Academy, Ankara-TURKEY
Hikmet Bayhan
Nuclear Medicine Department,
Gülhane Military Medical Academy, Ankara-TURKEY

Abstract

In this study, a new method called the pixel basis functional radionuclide imaging (PBFRI) algorithm based on the appended curve deconvolution technique, in order to be able to increase the medical diagnostic capability of a conventional gamma camera, is presented together with the clinical results. In the PBFRI method, retention function of each pixel is obtained from the renograms and cardiac curves generated by processing the filtered segments of the kidney and heart, using a special deconvolution method. The deconvolution operation is done by using the Fourier transform technique. High frequency artifacts presented by the Fourier transform are removed by using a novel method which is based on the use of the appended curves of raised cosine functions. The mean transit time (MTT) and the glomerular filtration rate (GFR) parameters are obtained from retention functions. Finally, the functional images related to MTT and GFR parameters are generated by pseudo coloring of different quantisation values in the range. Diagnosis of renal artery stenosis (RAS) is chosen as a clinical application of the proposed PBFRI method. It is shown that the PBFRI technique can be used as an alternative to existing digital subtraction angiography (DSA) in the diagnosis of RAS.

1. Introduction

Scintigraphic images provide useful information on the radioisotope distribution in the organs within the human body. Scintigraphic studies can be static or dynamic. Static images record the current intracorporal distribution of the radio indicator used. Dynamic imaging results by forming a sequence of scintigrams reflecting the changes in radioisotope transport, accumulation and elimination, with respect to time and location, within the organs. Dynamic renal scintigraphy is known as one of the essential tools in diagnosing the functional status and behaviour of the kidney [1,2,3].

In contrast with most static studies, dynamic studies have an inherently high noise level because of low count statistics [4]. Therefore, before attempting to generate pixel basis functional images relying

upon the raw data of a scintigraphic dynamic study, an effective technique must be sought for filtering out the impulsive and nonimpulsive noise components in that data [5]. In a previous study, an improved 3-D smoothing filter was applied to dynamic nuclear scintigraphic images for that purpose [6].

Deconvolution analysis has been frequently used in the assessment of renal function from the radionuclide scintigraphic images taken by a gamma-camera as the detection device [1,2,7]. A retention function which actually represents the impulse response of the kidney, is produced from the cardiac curve and the renograms which are generated by using the smoothed dynamic renal scintigraphic images. Retention function covering the spectrum of transit times through the kidney, can be used to obtain the reliable values of mean transit time (MTT) and glomerular filtration rate (GFR) which are two important renal functional parameters [8]. MTT and GFR parameters are derived from the retention function. The MTT is the average time for passage through the volume with respect to the bolus input of the radionuclide material at the renal artery. GFR is a parameter which is related to the filtration ratio. Filtration ratio is defined as the part of the kidney plasma flow transformed into the "filtrate". The value of the filtration ratio is 19% in normal kidneys. The quantity of the glomerular filtrate formed in 60 seconds in kidneys is called the GFR. The amplitude of the retention function at zero time gives a measure of the GFR.

Various transform techniques can be applied to perform deconvolution on the renograms [9, 10]. Matrices, curve fitting or constraint methods, orthogonal polynomials, and Fourier transforms are the common methods. Each of these methods has advantages and disadvantages.

The matrix method is easily implemented, but carries errors in the initial data points throughout the entire selection. This method also requires the input curves to be heavily smoothed before deconvolution.

Curve fitting or constraint methods produce good results, but require prior knowledge of the form of the good results.

In DOP (Deconvolution with Orthogonal Polynomials) algorithm there is a close relationship between noise level and polynomial degrees selected [10]. Since it is necessary to use higher number of polynomial degrees to cancel out the effects of noise, DOP algorithm is found to be a time-consuming approach [11].

The Fourier transform method is very straightforward and easy to implement, but causes high frequency artifacts when data is abruptly truncated.

In this study, a special deconvolution technique which incorporates the appended curves of raised cosine functions is used. The appended curve technique is a modification of the Fourier transform method, addressing artifacts caused by the abrupt termination of data. A new technique for constructing the pixel basis renal functional images of MTT and GFR parameters is defined. The proposed technique can clearly identify the functional status of a region consisting of approximately 10,000 nephrons out of 1,000,000 nephrons in the kidney. A deconvolution operation removes the factors which do not belong to the kidney from the renogram curve, and thus enhances the signal to noise ratio. The deconvolution operation is applied to both the input and output functions obtained from the regions of interest of the heart and the kidneys, respectively. Renal retention functions are extracted at the pixel basis level, and a retention function belonging to each pixel is used to evaluate the values belonging to MTT and GFR parameters. Finally, functional images of MTT and GFR parameters are obtained. Some clinical examples of their medical significance are also discussed in the manuscript. In addition, diagnosis of renovascular hypertension disease (RVH) due to the renal artery stenosis (RAS) has been taken as the clinical application of the PBFRI technique. Diagnostic capability of PBFRI has been assessed comparatively with respect to another well-known and widely used medical imaging technique known as the digital subtractive angiography (DSA).

The organization of the paper is as follows. Section 2 gives an overview of the symptoms and outcomes of the RAS disease, and briefly explicates and compares the imaging methods used in the diagnosis of RVH

arising from RAS. The proposed PBFRI method is detailed in Section 3. Section 4 describes how dynamic renal studies are performed, and extraction of MTT and GFR parameters using PBFRI method. In Section 5, some clinical examples are given, and the clinical application of the PBFRI method is described. Conclusions are drawn in Section 6.

2. Preliminaries

The main reason for the renovascular hypertension (RVH) developed due to the renal artery stenosis (RAS) is the increment in the plasma renin [12]. It is known that there is a renovascular factor in five percent of the patients having hypertension, and those patients can be treated by the help of percutaneous transluminal angioplasty (PTA) therapy technique. The diagnosis of RVH, precisely, has become an important goal especially after PTA [13].

In the case of unilateral RAS, glomerular filtration rate (GFR) and effective renal plasma flow (ERPF) increase in the other healthy kidney. The increase in GFR is greater than the increase in ERPF. But, the GFR value in the ischaemic kidney is kept constant since Angiotensin-II causes vasoconstruction in the efferent artery.

Preservation of GFR, while ERPF decreases, causes an increase in the filtration ratio. Therefore, transit time gets longer due to the increase in water and sodium absorbtion of the corresponding kidney.

Accumulation of fluid causes volume expansion in patients with a single kidney, or in the case of bilateral stenosis. The expanded volume decreases renin secretion in the stenotic kidney. In such patients, blood pressure increases due to the increased external cell volume, while plasma renin level stays at its own normal level. Even if the volume could be reduced, the blood pressure does not drop, since the renin secretion increases again. Hence, such patients have always hypertension because of volume expansion or too much renin secretion.

The most important difference between obstructive nephropathy and ischaemia is the longer duration of transit time in the pelvis region. Furthermore, there occurs an increase in GFR in the case of obstruction, while it does not change in ischaemia. In order to be able to distinguish obstructive nephropathy from ischaemia, pixel basis evaluation of MTT and GFR parameters should be known. These parameters are extracted from the functional images. Therefore, functional imaging of kidneys gains importance in differential diagnosis of obstructive nephropathy and ischaemia. Following results are obtained when the methods used for the diagnosis of RVH due to the RAS, are compared:

- "Correct diagnosis" performance of IVP method is poor (60% on the average). Therefore it cannot be used for diagnostic purposes [13].

- Detection of laterilisation in the stenotic kidney and taking renal venous renin sample is a reliable approach from the physiological point of view. "Correct diagnosis" performance of this technique is given as 74% in literature. Being invasive and having side effects are its disadvantages [13].

- Intra-venous digital subtraction angiography (IVDSA) is a reliable diagnosis technique with 90 percent sensitivity and "correct diagnosis" performance.

- Intra-arterial digital subtraction angiography (IADSA) is the best diagnosis technique but it has more side effects than IVDSA. A patient diagnosed as having RVH via IADSA is then treated using the PTA theraphy method. IADSA, which is called the "golden standart", is the most widely used method in the diagnosis of RVH.

On the other hand, radionuclide based techniques are also used in the diagnosis of RVH arising from RAS. The captopril test, which is an angiotensine converting enzyme inhibitor, is used in order to be able to increase the sensitivity of radionuclide based imaging techniques [14, 15]. Captopril test is also used in RVH for diagnostic purposes, since GFR decreases in stenotic kidney after the test. Due to the differences in physio-pathological mechanisms causing hypertension, bilateral stenosis and single stenotic kidney do not respond to captopril test, while unilateral stenosis responds easily to the same test [16-18]. When the renogram curves are observed after the captopril test is performed, shapes of the curves and the duration of reaching the peak value carry important information for the diagnosis of RAS [14, 15].

Pixel basis renal functional radionuclide imaging technique, proposed in this study, is as reliable as the DSA method. It will be shown in following sections that it can be used in the diagnosis of both unilateral and bilateral RAS diseases.

Furthermore, PBFRI technique is noninvasive, easy to use, and inexpensive compared to DSA.

3. Pixel Basis Functional Radionuclide Imaging (PBFRI) Method

As the first step of our approach, five regions of interest, one over each kidney (renal ROIs), one below each kidney (background ROIs), and one over the heart (cardiac ROI) are traced and smoothed by the 3-D smoothing filter (see Fig. 1).

Figure 1. Regions of interest used in the PBFRI method.

A background curve is generated by summing the pixel values in the background ROI, and dividing by the number of pixels. This can be considered to consist of two components, the extra-renal background which is partly vascular and partly extravascular B_{F1}, and the intra-renal vascular background B_{F2} [19].

The cardiac curve $C'(t)$ in Fig.2, is generated similarly by summing pixel values in the cardiac ROI containing blood arteries near the kidney. The cardiac curve is then background subtracted using a factor of 0.57 of the background [20].

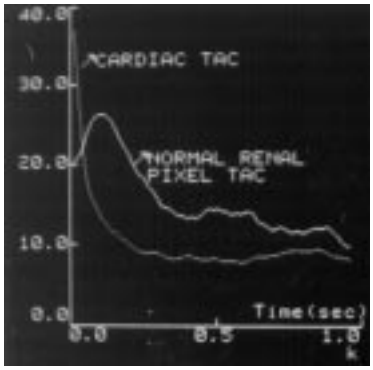

Figure 2. Cardiac and renal pixel time activity curves (TAC).

$$C(t) = C'(t) - 0.57B_{F1} \tag{1}$$

The variation in the count rate of each pixel with time obtained over the renal ROI can be represented by $\mathrm{R}_\alpha(\mathrm{t})$. The smoothed renogram curves of each pixel includes the extra-renal background component multiplied by a factor of 0.8 [1].

$$R_\alpha(t) = K_\alpha(t) + 0.8B_{F1} + B_{F2} \tag{2}$$

where $\mathrm{K}_\alpha(\mathrm{t})$ represents the variation of activity in the renal ROI tissue pixel and α is the pixel number.

The background corrected renogram curve of each pixel $\mathrm{K}_\alpha(\mathrm{t})$ in Fig. 2, is a convolution of the cardiac curve C(t), and the retention function $\mathrm{H}_\alpha(\mathrm{t})$, of the related pixel in the kidney. Factors of 0.57 and 0.8 in Eq. 1 and Eq.2, respectively, are empirical coefficients and they are commonly used in nuclear medicine [1], [20].

$$K_\alpha(t) = C(t)^\star H_\alpha(t) \tag{3}$$

The main assumption made in this approach is that the kidney can be modelled as a linear, time-invariant system with zero initial state. From a practical point of view, the last part of this assumption implies that there is no residual radioactive material in the blood of the patient at the beginning of the study.

A sum of renogram and extravascular contribution is

$$R'_\alpha(t) = C(t)^\star H_\alpha(t) + B_{F2}.C(t) \tag{4}$$

If $\mathrm{R}'_\alpha(\mathrm{t})$ is deconvolveld with C(t), the result becomes

$$H'_\alpha(t) = H_\alpha(t) + B_{F2} \star \delta \tag{5}$$

where δ is the delta function. Subtraction of $\mathrm{B}_{F2} \star \delta$ from the resultant vector $\mathrm{H}'_\alpha(\mathrm{t})$ yields the retention function of each pixel $\mathrm{H}_\alpha(\mathrm{t})$.

A deconvolution technique based on the appended curves of raised cosine functions is used on the pixel basis cardiac and renogram curves. A raised cosine function, $\mathrm{F}_{APP}(\mathrm{n})$, 2-3 times the length of the initial acquisition is appended to the tails of both of the input curves as given below (Fig.3):

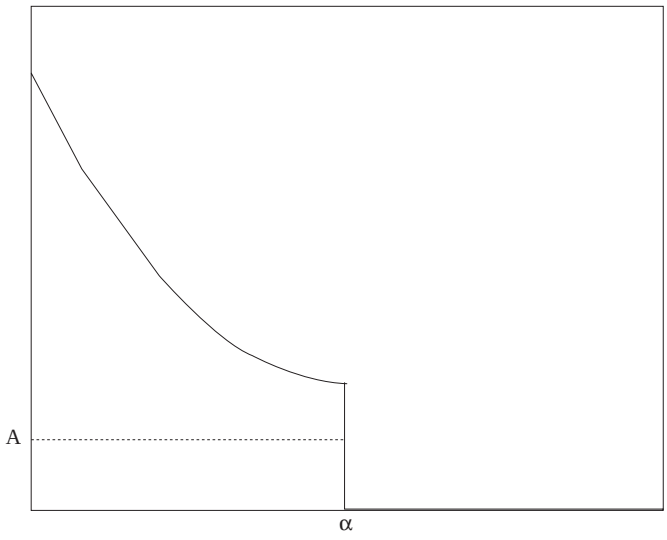

(a)

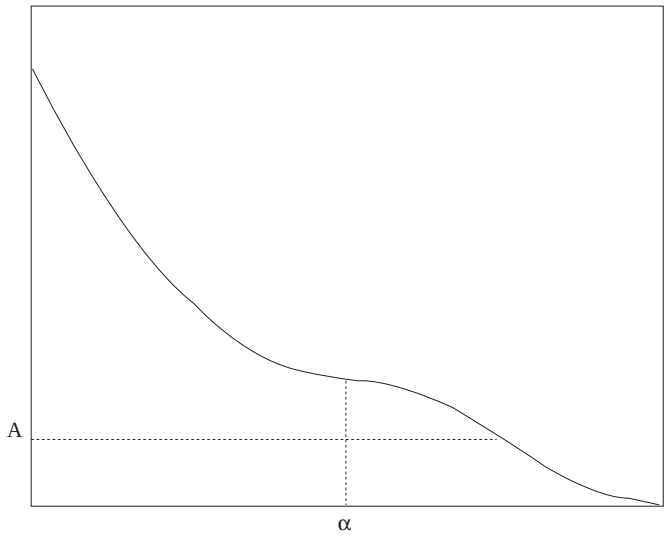

(b)

Figure 3. (a) Blood pool curve, C(n), (b) Blood pool curve after the raised cosine function is appended, C'(n).

$$C'(n) = C(n) + F_{APP}(n) \tag{6}$$

where

$$F_{APP}(n) = \begin{cases} 0 & 0 \leq n \leq \alpha \\ A(1 + \cos(\pi \frac{(n-\alpha)}{(N-\alpha)} & \alpha < n < N \end{cases} \tag{7}$$

In Eq. (7) $N=2^j$, j=0,1, ..., K and α <N. This appended curve will gradually taper the input curves to zero, removing high frequency components caused by the sudden termination of the acquisition.

The discontinuity in these time activity curves (TAC) is caused by the abrupt termination of the acquisition. A raised cosine function is appended to the end of each curve to gradually bring it down to zero. This appended curve lengthens the original curve several times.

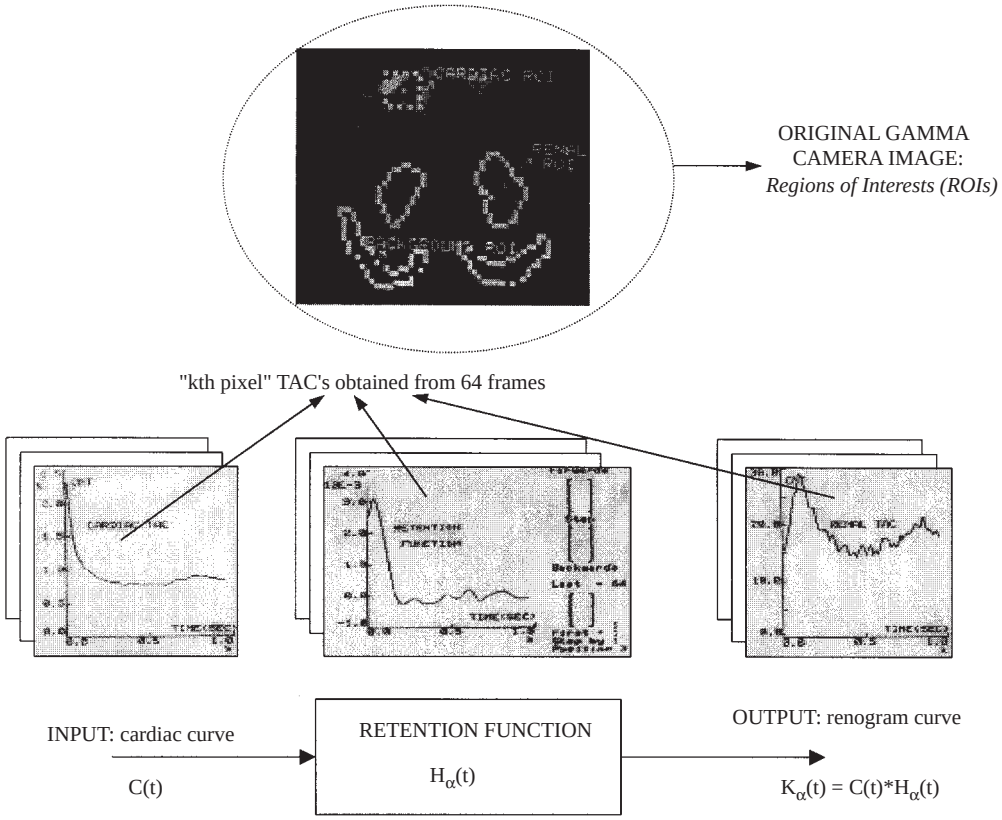

Figure 4. Modelling of the kidney using the deconvolution method, and time activity curves of the system. C(t): Background subtracted cardiac curve, $H_\alpha(t)$: Retention function, $K_\alpha(t)$: Renogram curve of each pixel. TAC: Time Activity Curve.

The Fourier transforms of both curves are determined. The renogram curve is divided by the cardiac curve in frequency domain and the inverse Fourier transform is taken.

Since each of the input curves is appended with a raised cosine function, neither of the input curves needs to have a number of points equal to a power of two. The appended number of curve points will always be a power of two.

In the complex divide routine a "divide by zero" is defined to equal zero. The appended curves also take care of wraparound problems. The end of the raised cosine function is essentially zero for approximately the length of the original input curve.

Each appended curve is checked to see if the total number of curve points is a power of two. If necessary, zeroes are appended so that the total number of points in each curve is a power of two.

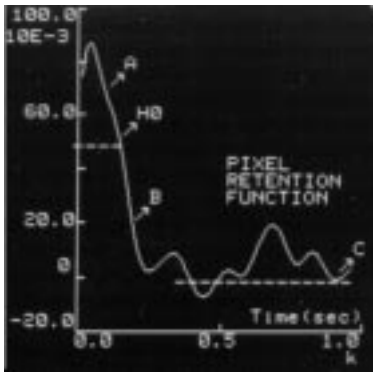

Figure 5. Renal pixel retention function

Modelling of the kidney in the deconvolution method, and the time activity curves (TAC) of the system are shown in Fig. 4. As mentioned in Section 1, MTT and GFR parameters are derived from the retention function. The steps in this deconvolution method are as follows:

- Append raised cosine function to the tails of the cardiac and renogram curves.
- Perform an FFT on the appended cardiac and renogram curves.
- Divide renogram curve by cardiac curve in frequency space.
- Perform an inverse FFT ont the resulting curve.
- Remove extra points from the tail of the deconvolved curve.

Early uptake of Diethylene Triamine Pentaacetic Acid (DTPA) is proportional to GFR that is why the amplitude images represent the regional distribution of GFR. From Equation (8), MTT values of each pixel are obtained in minutes.

$$MTT = (H_0.60)^{-1} \sum_{n=1}^{k} H_n.\Delta t \tag{8}$$

where k represents the element in H corresponding to the maximum transit time, H_0 is the amplitude of the retention function at zero time, Δt is the time-interval between frames.

H_0 is the average plateau value in the pixel retention function in Fig.5. All the values from the plateau start point through the plateau end point are summed and divided by the number of points in the plateau to yield the average plateau value. The plateau start point is found by searching for the first point greater than 90% of Y_{max} (Point A). If there is no point less than Y_{max} at the start of the curve, then the plateau start is set to the first point. The plateau end point is found by searching from Y_{max} for the first point less than 90% of Y_{max} $(PointB)$. If there are no points higher than the average plateau value, then MTT is calculated up to second negative going zero crossing defined as point C (see Fig.1). If another peak is found exceeding the plateau value at one of the next frames, a new retention function is constructed by extrapolation of this maximum back to the zero time.

For a pixel placed at the periphery of the kidney, the arrival of the radionuclide material in renal artery to the pixel volume is virtually instantaneous and the retention function will be a monotonically decreasing

function. That is why the above MTT formula can be applied directly. However, for a more central pixel, the total activity is partially affected by the collecting system and the arrival is not instantaneous. The retention function first rises to a maximum and then falls as the bolus passes through the pixel volume. For this case, the mean transit time is calculated as explained in the previous paragraph.

4. Method

Dynamic renal studies are performed with ^{99m}Tc-DTPA. DTPA labelled with ^{99m}Tc constitutes an agent with suitably sized molecules to be cleared in a truly glomerular manner by the kidneys.

The patient is hydrated and gamma camera renography is carried out with the subject in a seated position using intravenous injection of 5 millicurie ^{99m}Tc-DTPA. Then, data consisting of 64 frames of 64×64 pixels each, are smoothed by the 3-D smoothing filter [6].

The background subtracted cardiac values and renograms of each pixel obtained from the filtered dynamic renal scintigraphic images are used as the time activity curves of 15 seconds time interval covering the first 16.6 minutes of acquisition. Finally, functional images related to MTT and GFR parameters are created by using the pixel-basis PBFRI method. These images are generated by pseudo colouring of the different quantization values in the range (See Figs. 6, 7, 8 and 9).

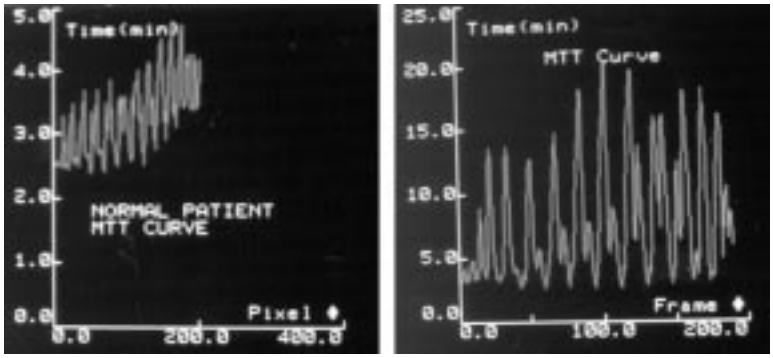

Figure 6. MTT curves for (a) a normal patient, (b) an obstructed patient

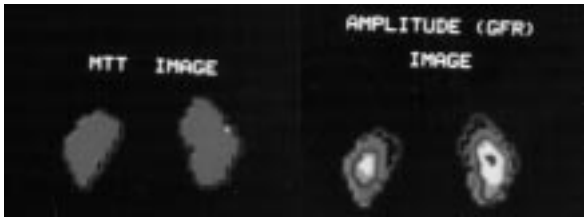

Figure 7. MTT and GFR images for a normal patient.

Figure 8. MTT and GFR images for a bilateral obstructive uropathy patient.

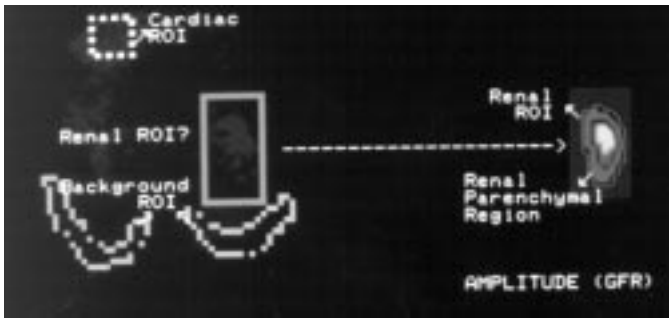

Figure 9. Automated renal and parenchymal regions of interest selection.

Table 1. Color translation table for mean transit time images

MTT (min)	Color
<2.00	Yellow
2.00 - 2.50	Light Brown
2.50 - 3.50	Green
3.50 - 4.50	Dark Green
4.50 - 6.50	Light Blue
6.50 - 8.50	Blue
8.50 - 12.00	Purple
12.00 - 16.00	Dark Purple

5. Results and Discussion

5.1. Examples on the Evaluation of GFR and MTT Parameters

By using the PBFRI method, MTT and GFR values attain an easily perceptable medical meaning to indicate the physiological status of each pixel volume, in the form of functional images. On the other hand, parenchymal region, collecting system and pelvis are determined with greater accuracy in comparison to the other conventional techniques. The MTT images clearly provide information on the regional transit of chelate through the kidney at pixel accuracy. In clinical practice this is particularly useful in determining the exact extent at which the delay is occuring and the amount of parenchyma remaining with normal transit time.

For a normal patient, the MTT values are found in the range of 2.5 to 4.5 minutes with values increasing from the periphery towards the pelvis (see Fig. 6(a)).

For a patient who has obstructive uropathy, these values go up to 9 minutes (see Fig.6(b)). Pelvis and collecting system of these two kidneys have high MTT values.

By using the pixel basis RFRI method, the functional images of the renal MTT and GFR parameters are also obtained accurately. The normal and obstructed MTT and GFR image patterns in Fig.7 and Fig.8 respectively, show a smooth variation of image density reducing towards the edges. Notice that at amplitude (GFR) image in Fig.9, localized areas of abnormality have decreased the amplitude values. By increasing the contrast of amplitude (GFR) images, it becomes very easy to locate renal and parenchymal regions for ROI selection of further studies (see Fig.9).

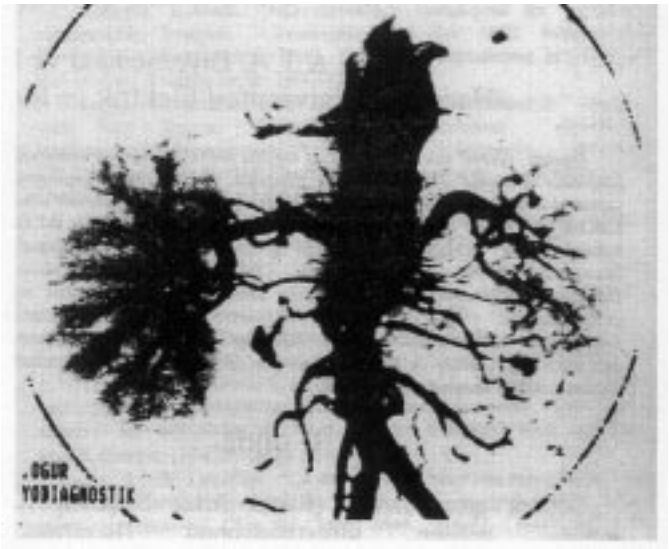

Figure 10. Angiogram image of the patient having bilateral RAS.

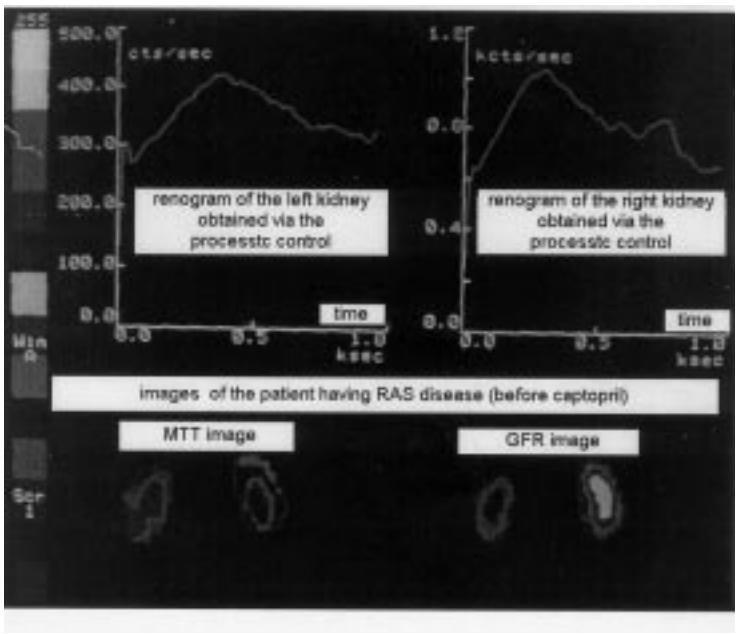

Figure 11. Conventional renogram curves, and RFRI based functional images from the left and right kidneys of the patient having bilateral RAS (before captopril test.)

6. Clinical Application of the PBFRI Method

In the clinical application of the PBFRI method, subjects included one patient having bilateral RAS, and another one with a single transplanted kidney having unilateral RAS. Diagnoses were confirmed with the intra-arterial digital subtraction angiography (IADSA) technique. Proposed PBFRI method was then applied to the patients' dynamical scintigraphic images recorded before and after the captopril test. Results obtained

via the PBFRI were then compared to the renography technique that is used for diagnostic purposes in such clinical applications.

In the conventional renography method, shapes of the renogram curves, before and after the captopril test, are observed. A patient is diagnosed as having RAS, if there occurs a decrease in the pre-captopril excretion phase while a smoothing occurs after the captopril in the renogram curves.

By using the DSA method, it was found that the patient having renovascular hypertension (RVH) due to the bilateral stenosis, have 80% and 50% levels of RAS in left and right kidneys, respectively (Fig. 10). Functional MTT and GFR images obtained using the PBFRI technique, and standart renogram curves before captopril was applied, are depicted in Fig. 11. Fig. 12 shows functional images and renogram curves obtained after captopril.

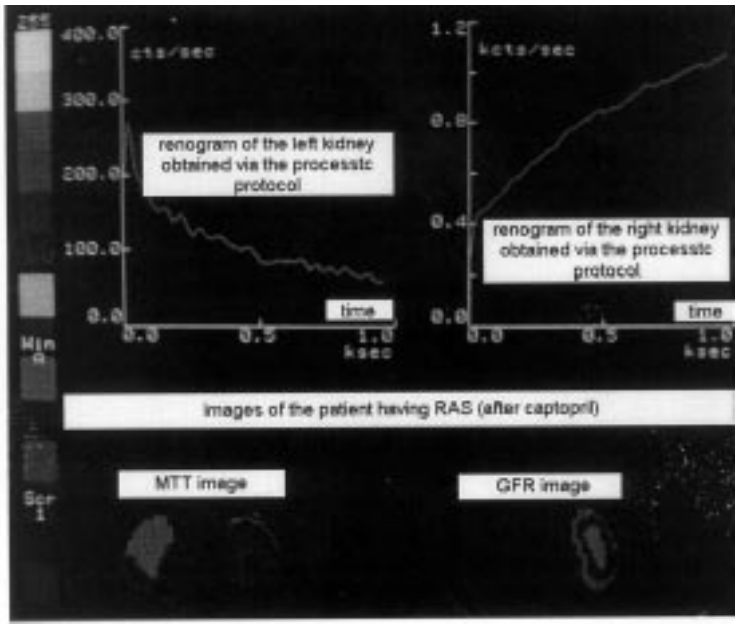

Figure 12. Conventional renogram curves, and RFRI images from the left and right kidneys of the patient having bilateral RAS (after captopril test).

When the renogram curves from both kidneys were observed, a resemblance to the shapes of the curves obtained from patients having obstruction was noticed. Therefore, it was concluded that the renogram curves cannot be used in differential diagnosis of ischaemia and nephropathic obstruction. But, when MTT and GFR images of the left kidney were analysed visually, it was found that the MTT values were 10 minutes on the average in one region of parenchyma while they were changing in between 5 and 8.5 minutes in the remaining regions. MTT values were almost normal in the right kidney, i.e., the change was in 5-10 minutes range in the pelvis region and in the collecting system. MTT values in pelvis regions of both kidneys were close to the MTT values obtained from the other regions. On the other hand, change in GFR was lower than expected, in the left kidney while the change in GFR values in the right kidney was almost normal. Therefore, using also the MTT functional images, this patient can be diagnosed as having the RAS disease. It should be emphasized that the patient was given 50 mg of captopril two days after the images were recorded without captopril, and PBFRI method was applied to those images.

When the renogram curves were observed after captopril, it was noticed that the left kidney immediately passes to excretion phase, while renogram curves belonging to the right kidney became straight during

the same phase. It was also noticed from GFR and MTT images that, GFR values belonging to the left kidney dramatically dropped down after captopril. As a result of this situation, MTT values got shorter. The reason for that is a rapid blood passage through the left kidney without any uptake. Therefore, there is no glomerulary filtration in this kidney, and the right kidney performs the filtration alone. In the right kidney, as expected, MTT values got longer while GFR values decreased. On the other hand, a long MTT value of which the pelvis region could be discriminated from other regions, could not be found in both kidneys. All of these findings confirm the diagnosis of RAS and its level for both of the kidneys.

By using the DSA method, it was found that the patient with a single transplanted kidney having hypertension has RAS of 50% in level. This patient's angiogram image is shown in Fig. 13. Functional MTT and GFR images obtained using the PBFRI technique, and standard renogram curves before captopril, are depicted in Fig. 14. Fig. 15 shows functional images and renogram curves obtained after captopril was applied to the same patient.

When Fig. 14 was observed, it was noticed that, the renogram curve of the patient with a single transplanted kidney is similar to the renogram curves which could be extracted from the patients having obstructive nephropathy. While MTT values were changing in between 3.5 and 4.5 minutes in parenchyma, values up to 8.5 minutes were found in the collecting system, and in the pelvis region. Unlike the other regions of kidney, MTT values did not get longer in the pelvis region. On the other hand, GFR values were similar to the GFR values of a healthy kidney. Therefore, it was concluded that the patient could be diagnosed as having the RAS disease.

When the renogram curves were observed after captopril (Fig. 15), it was noticed that there exists an increase in the excretion phase, and in MTT values, while GFR values were decreasing. This was an expected situation. In conclusion, GFR values were found to be normal, and MTT values got longer in the parenchymal region before captopril, while, after captopril, GFR values decreased, and MTT values increased especially in the parenchymal region and in the collecting system. This examination shows that there is a parallelism between the findings of IADSA and PBFRI techniques.

Figure 13. Angiogram image of the patient with a single transplanted kidney having RAS disease.

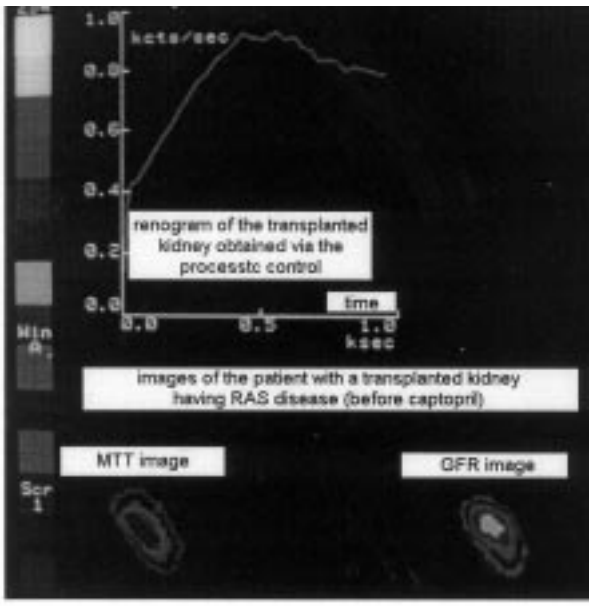

Figure 14. Conventional renogram curves, and RFRI based functional images of the patient with a single transplanted kidney having RAS disease (before captopril test).

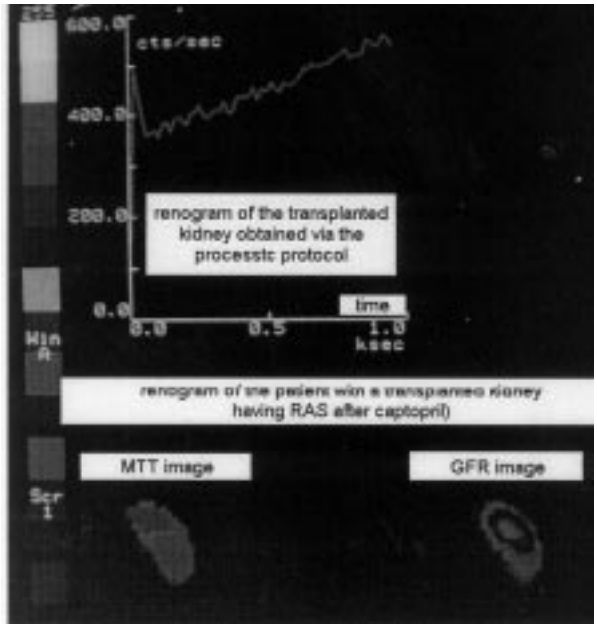

Figure 15. Conventional renogram curves, and RFRI based functional images of the patient with a single transplanted kidney having RAS disease (after captopril test).

In conclusion, our clinical study showed that the functional MTT and GFR images obtained via the PBFRI technique

- carry valuable information for the objective evaluation and diagnosis of unilateral and bilateral RAS disease,
- can be used to determine the local effects of RAS, and
- avail us of the possibility to observe the local changes in MTT and GFR values in both kidneys.

7. Conclusions

In this work, a method which can be used to obtain the pixel basis functional images of MTT and GFR functional parameters is proposed. The most important contribution of the proposed method is that the pixel basis approach avails the user of the possibility to observe the regions of interest in kidneys with higher resolution than the conventional nuclear imaging techniques. Conventional techniques result in global curves which give an insight about the whole kidney consisting of approximately 1,000,000 nephrons of which each has its own filtration capability. On the other hand, functional images obtained via the proposed PBFRI technique avail the user of the possibility to zoom in and observe 10,000 nephrons. The deconvolution operation used in the PBFRI method is enacted by a Fourier transform based technique which is easy to implement, and computationally faster than the deconvolution with orthogonal polynomials or matrix implementation. But, Fourier transform causes high frequency artifacts especially when the data is abruptly truncated. This disadvantage has been overcome by using the appended curves of raised cosine functions. In this method, a raised cosine function is appended to the end of each curve in order to bring it gradually to zero.

By using this PBFRI method, it is possible to determine one sided and two sided renal arter stenosis in the renovascular hipertensive patients by looking at the transit times and amplitude values of each pixel in the parachimal region, collecting system and pelvis. At the same time, the regional effects of renal arter stenosis can be determined by looking at the pixel basis regional variations of MTT and GFR values.

The main difference between the renal arter stenosis and urinary tract obstruction is at the lengths of transit times in the pelvis. In the urinary tract obstruction, GFR values decreases, but this parameter does not change in the renal arter stenosis. On the other hand, in the renovascular hypertension, paranchymal transit time inreases. As a result, in order to differentiate and diagnose the renal arter stenosis and urinary tract obstruction accurately, the PBFRI method can be the unique and the fastest method, which can be applied by a conventional gamma camera.

Urinary tract obstruction can be acute, chronic, partial or complete, progressing or improving. In a "functioning" kidney, the radiology can often demonstrate the existence of obstruction and indicate, usually, its level. But from radiological data, it is not possible to make statements regarding renal function or the moments at which active intervention should occur. Such intervention in acute cases, in general, results in functional and morphological normality. In the PBFRI method, by means of the MTT and GFR images, it is also possible to determine the degree of obstruction in this kind of pathological case.

8. Acknowledgement

Authors would like to thank Dr. Emel Sabuncu Öztürk of the Nuclear Medicine Department of Gülhane Military Medical Academy, for her kind help during the whole study, and Dr. Erkin Oğur of the Radiology Department of Gülhane Military Medical Academy, for his invaluable contribution.

References

[1] Kenny, R. W., Ackery, D. M., Fleming J. S., Goddard, B. A. and Grant, R. W. (1975) Deconvolution of the Scintillation Camera Renogram. *British Journal of Radiology,* vol. 48, pp. 481-486.

[2] Diffey, B. L., Hall, F. M., Corfield, J. R. (1976) The ^{99m}Tc-DTPA Dynamic Renal Scan with Deconvolution Analysis. *J. Nucl. Med.,* vol. 17, pp. 352-355.

[3] Piepsz, A., Ham, H. R., Erbsmann, F., Diffey, B. L., Goggin, M. J., Hall, F. M., Lumbroso, J., Paola, R. and Bazin, J. P. (1982), A Co-Operative Study on Clinical Value of Dynamic Renal Scanning with Deconvolution Analysis, *British Journal of Radiology*, vol.55, pp.419-433.

[4] Sorenson, J. A. and Phelps M. E. (1980) Physics in Nuclear Medicine. New York: Grune and Stratton, ch. 6, pp. 100-114.

[5] Pokropek, A. T. and Paola, R.Di (1982) The Use of Computers for Image Processing in Nuclear Medicine. *IEEE Trans. Nucl. Sci.,* vol. NS-29, pp. 1299-1309.

[6] Karagöz, İ. and Eroğul, O. (1999) A New 3-D Double Window Adaptive Hybrid Smoothing Algorithm and its Applications on Radionuclide Images. *Journal of Imaging Science and Technology,* vol. 43, no. 2, pp. 133-137.

[7] Bajén, M. T., Puchal, R., González, A., Grinyó, J. M., Castelao, A., Mora, J., Comin, J. M., (1997) MAG3 Renogram Deconvolution in Kidney Transplantation: Utility of the Measurement of Initial Tracer Uptake. *J. Nucl. Med.,* 38, 1295-1299.

[8] Kempi, V., Sutton, D. G. (1995) Estimating the Diagnostic Yields Resulting from Renography and Deconvolution Parameters: A Logistic Regression Analysis, *J. Nucl. Med.,* 36, 147-152.

[9] Huffel, S. V., Vandewalle, J., De Roo, M. Ch., Willems, J. L. (1987) Reliable and Efficient Deconvolution Techniques Based on Total Linear Least Squares for Calculating the Renal Retention Function. *Med. and Biol. Eng. & Comput.,* vol. 25, pp. 26-33.

[10] Stritzke, P., King, M. A. and Vaknine, R., S. J. Goldsmith, 1990, Deconvolution Using Orthogonal Polynomials in Nuclear Medicine: A Method for Forming Quantitative Functional Images from Kinetic Studies, IEEE Trans. on Medical Imaging, vol. 9, pp. 11-23.

[11] Karagöz, İ., Akata, E., (1991) Applications of Deconvolution Algorithms and Smoothing Techniques to Renal Functional Images, in Computer Assisted Radiology (CAR), Springer-Verlag, Berlin, pp.824.

[12] Brunner, H. R., Waeber, B., Nussberger, J., (1989) The renin System Hypertension, *Radionuclides in Neprology,* London, 1-6.

[13] Tack, C., Sos T. A., (1989) Radiologic Diagnosis of Renovascular Hypertension and Percutaneous Transluminal Renal Angiography, *Sem. Nucl. Med.,* 19, 89-94.

[14] Gijsbert, G., Oei, M. Y., Puylaert, C. B. A. J., Mees, E. J. D., (1986) Renography with Captopril, *Arch. Intern. Med.,* 146, 1705-1708.

[15] Kletter, K., (1988) Captopril Renography in Goldblatt Hypertension, *J. Nucl. Med.,* 29, 87-94.

[16] Lee, H. B., Blaufax, M. D., (1989) Renal Functional Changes after Converting Enzyme Inhibition or Nutroprusside in Hypertension with Captopril in Rats, *J. Nucl. Med.,* 29, 509-515.

[17] Lee, H. B., Blaufax, M. D., (1989) technetium-99m MAG-3 Clearances after Captopril in Experimental Renovascular Hypertension with Captopril in a Rat Model, *J. Nucl. Med.,* 29, 509-515.

[18] Nally, J. V., Clarhe, H. S., Grupta, B. K., Grecos, G. P., Gross, M. L., Potvin, W. J., Windham, J. P., (1987) Captopril Challenge with Radionuclide Assessment in Two kidney and One Kidney Goldblatt Hypertension, *Bischof-Delaloye*, London, 95-103.

[19] Taylor, A., Thakore, K., Folks, R., Halkar, R., Manatunga, A. (1997) Background Subtraction in Technetium-99m-MAG3 Renography. *J. Nucl. Med.,* 38, 74-79.

[20] Fleming, J. S. (1977) Measurement of hippuran plasma clearance using a gamma camera. *Phys Med Biol,* vol. 22, pp. 526-530.